water

MDPI

Article

Mechanism of Biological Transport and Transformation of Copper, Cadmium, and Zinc in Water by *Chlorella*

Shaomin Liu [1,2,*], Mengyu Jiang [1], Jiating Wu [1], Xiaofeng Li [1] and Jinglin Zhu [1]

[1] School of Earth and Environment, Anhui University of Science and Technology, Huainan 232001, China; 19855680502@163.com (M.J.); wu15155442086@163.com (J.W.); 13023094026@163.com (X.L.); jlzhu@aust.edu.cn (J.Z.)
[2] State Key Laboratory of Mining Response and Disaster Prevention and Control in Deep Coal Mines, Anhui University of Science and Technology, Huainan 232001, China
* Correspondence: shmliu1@163.com

Abstract: This study investigates the effectiveness of *Chlorella vulgaris* in treating copper, cadmium, and zinc in aqueous solutions; the aim of this study was to examine the effects of various factors on the adsorption capacity of Chlorella in water. This study explored the intra- and extracellular adsorption and accumulation patterns of copper (Cu(II)), cadmium (Cd(II)), and zinc (Zn(II)), revealing their molecular response mechanisms under the most suitable conditions. The adsorption capacity of Chlorella to Cu(II), Cd(II), and Zn(II) in water was 93.63%, 73.45%, and 85.41%, respectively. The adsorption mechanism for heavy metals is governed by both intracellular and extracellular diffusion, with intracellular absorption serving as a supplement and external uptake predominating. XRD, XPS, FTIR, SEM-EDX, and TEM-EDX analyses showed that there would be the formation of precipitates such as Cu_2S, CuS_2, CdS, and $ZnSO_4$. The adsorption of Cu(II) involves its simultaneous reduction to Cu(I). Moreover, specific functional groups present on the cellular surface, such as amino, carboxyl, aldehyde, and ether groups, interact with heavy metal ions. In view of its efficient heavy metal adsorption capacity and biosafety, this study recommends Chlorella as a potential biosorbent for the bioremediation and environmental treatment of heavy metal contaminated water in the future.

Keywords: water; *Chlorella vulgaris*; bioabsorption; transformation form; copper/cadmium/zinc

Citation: Liu, S.; Jiang, M.; Wu, J.; Li, X.; Zhu, J. Mechanism of Biological Transport and Transformation of Copper, Cadmium, and Zinc in Water by *Chlorella*. *Water* **2024**, *16*, 1906. https://doi.org/10.3390/w16131906

Academic Editor: Md Abu Hasan Johir

Received: 23 May 2024
Revised: 20 June 2024
Accepted: 23 June 2024
Published: 3 July 2024

1. Introduction

Water is one of the essential elements for life on Earth [1]. Nowadays, the quality of water is affected by a variety of harmful pollutants in water, some of which are produced by industrial and mining activities, such as cadmium (Cd), chromium (Cr), copper (Cu), nickel (Ni), zinc (Zn), lead (Pb), and mercury (Hg) [2]. These pollutants are highly carcinogenic, mutagenic, and toxic, which can lead to various changes in plants, animals, and humans, causing environmental and human health problems [3,4]. Heavy metal ions have been identified as the most serious contributor to wastewater contamination, mainly because of their accumulation and spread through the food chain, posing a grave threat to human health and ecosystems, as well as to their toxic and non-biodegradable characteristics [5]. Among these heavy metals, Cu(II), Cd(II), and Zn(II) are categorized as three important pollutants. High levels of copper and zinc have been shown to damage the liver and induce nausea, vomiting, diarrhea, and abdominal pain, while excessive zinc can impair immune responses [6,7]. Cadmium is not only one of the heavy metals that most severely impact aquatic life but also one of the most toxic pollutants to phytoplankton [8]. The impact of cadmium extends beyond aquatic ecosystems, contributing to cell death, as well as the onset of kidney and bone diseases, along with impairment in lung function [9–11]. Research has shown that pollutants related to heavy metals are hard to remove [12]. Therefore, wastewater containing heavy metal pollution has received extensive research attention, and the development of effective methods to remediate heavy metal ions in wastewater

has become crucial. It becomes imperative to prevent the release of Cu, Cd, and Zn ions into the environment by employing efficient removal processes before discharging them into the surroundings.

Studies have shown that heavy metals in wastewater can be removed by membrane filtration [13], solvent extraction [8], chemical precipitation [14], ion exchange [15], and adsorption [5]. In recent years, there has been a shift towards the use of biological methods for heavy metal removal due to the low cost and environmentally friendly nature of microbial cultivation. In particular, microalgae have simple structures, rapid growth rates, and high photosynthetic efficiency and, thus, are judged to be potential candidates for heavy metal treatment. They can remove heavy metals through mechanisms such as remediation and bio-adsorption, achieving higher removal efficiency [8]. Furthermore, relevant research has demonstrated that microalgae are effective in removing heavy metals. They are environmentally friendly, easily assimilated, and capable of bioremediation [16,17]. Among them, Chlorella is one of the more relevant microalgae and can survive in a variety of environments, including mines and industrial waters [16,18]. Furthermore, relevant studies have indicated that Chlorella can tolerate a number of different heavy metal ions, including Zn(II), Cu(II), Ni(II), or Cd(II) [19,20]. Zhao et al. [5] showed that the adsorption rates of Cd and Cu were as high as 95% and 99%, respectively, using a novel Dielectrophoresis-assisted device for the bioremediation of heavy metal ions using *Chlorella vulgaris* at a concentration of 1.65 g/L. The results showed that the adsorption rates of Cd and Cu were as high as 95% and 99%, respectively, by *Chlorella vulgaris*. The bioremediation of individual heavy metal ions in wastewater by *Chlorella vulgaris* was shown to be excellent. James et al. [21]. compared the removal efficacy of two algal species, *Chlorella vulgaris* and Scenedesmus obliquus, for Cd and Cu in water and showed that *Chlorella vulgaris* was a more effective adsorbent for the two metals compared to *S. obliquus*, both in single and mixed metal solutions, and its binding capacity for both metals was also higher. Chlorella has significant advantages over other similar species in the adsorption of heavy metals in water, including strong adsorption capacity, high efficiency, fast adsorption rate, high tolerance and survivability, environmentally friendliness, and low cost, as well as diverse adsorption mechanisms. These advantages make Chlorella a promising candidate for heavy metal contamination treatment and are of great value for research.

The process of algae adsorbing heavy metals is relatively complex and generally divided into two stages [22]. The first phase is extracellular adsorption, a process that is rapid and considered passive. This adsorption occurs immediately after contact with the metal and involves mechanisms such as the interaction of metal cations with the anionic cellular ligands, formation of microprecipitates, surface complexation, as well as covalent connections between proteins and other polymers and metal ions. Intracellular accumulation, the second phase, is thought to be active even though it moves more slowly than the first. The mechanisms involved exhibit species-specific characteristics, exemplified, for example, by the formation of metal chelates by plant chelating agents. Heavy metals are bound into algal vesicles, which then bind to proteins, DNA, and lipids [23]. Microalgae are efficient adsorbents/accumulators of heavy metals in acidic mine wastewater [24], and they can either adsorb or actively translocate heavy metals through cell organization. The mechanism involves the interbinding of metal ions with negatively charged characteristic groups on the cell surface, followed by accumulation within vacuoles [25]. In both phases, the cell surface attracts some of the metals to be bound, and inside the cell, there is a buildup of metals due to the different types of metals as well as differences in the algae themselves [26]. Surface adsorption is the most important aspect of the adsorption process as it constitutes the majority of it [27]. Nevertheless, the relative significance of surface adsorption for metals and algae may differ [26]. However, the distribution and morphological changes in heavy metals in algal cells remain to be explored. Therefore, exploring the distribution of heavy metals within and external to microalgal cells, alongside the response mechanisms of active compounds during the immobilization of heavy metal ions, is essential to elucidate the mechanism of heavy metal immobilization in microalgae. This comprehensive examination

aims to clarify the immobilization mechanism of heavy metal ions in microalgae, thereby establishing a theoretical foundation for a deeper understanding of the intricate interplay between microalgae and heavy metals. Such insights are pivotal for advancing strategies that ensure the safe disposal and resource utilization of heavy metals.

Based on the above questions, to study the ability of *Chlorella vulgaris* to adsorb Cu(II), Cd(II), and Zn(II), *Chlorella vulgaris* was subjected to different initial concentrations of pH and heavy metal ions in order to obtain the most adapted adsorption conditions for *Chlorella vulgaris*. By employing kinetic and isotherm models, FTIR (Fourier Transform Infrared Spectroscopy) and XPS (X-ray Photoelectron Spectroscopy), as well as quantifying the content of reduced glutathione (GSH) in algal systems, the adsorption process of microalgae was elucidated. The morphology before and after algae adsorption was analyzed using XRD (X-ray Diffraction), SEM (Scanning Electron Microscopy), TEM (Transmission Electron Microscopy), and EDX (Energy Dispersive X-ray Spectroscopy). Additionally, the amount of adsorption intracellular and extracellular was measured to reveal the synergistic mechanism between microalgae and heavy metal ions. In conclusion, this study elucidated the synergistic mechanism of heavy metal adsorption by Chlorella; clarified the transformation and migration mechanism of heavy metals in Chlorella, as well as the response mechanism of related active substances to immobilization; and laid a theoretical foundation for further studies on the interaction between microalgae and heavy metals.

2. Materials and Methods

2.1. Chlorella

2.1.1. Chlorella Culture

The microalgae *Chlorella vulgaris* (CV) utilized in this experiment was acquired from the Freshwater Algal Culture Repository of the Institute of Hydrobiology, Chinese Academy of Sciences. The preliminary culture was conducted in a sterile BG11 medium (Table S1) in a GY-FYQ-1564-ZZ-type photobioreactor (LeadingTec®, Wenzhou, China), with a temperature maintained at 30 °C (12:12 light-dark cycle) and an airflow rate of 15 L/h. The Chlorella were cultured until they entered the stable phase, characterised by a cell number increase of no more than 5% per day. The initial density of Chlorella was approximately 1.0×10^8 cells/mL, as measured by cytometry. Subsequent experiments were performed after the Chlorella reached a stable growth phase.

2.1.2. Determination of Standard Curves and Microalgae Concentrations

Four clean 500 mL conical flasks, four clean 50 mL plastic centrifuge tubes, a bottle of Chlorella in the logarithmic growth phase, and several volumes of BG11 culture solution were taken. Four plastic centrifuge tubes were weighed, and their initial masses were recorded. Subsequently, we diluted the logarithmic-phase microalgae solution with BG11 culture solution and distributed the dilution into four 500 mL conical flasks. The absorbance (OD660) of the algal solution in the four conical flasks was adjusted to 0.1, 0.2, 0.3, and 0.4, as measured by UV-visible spectrophotometer (Shanghai Hengping UV-Vis Spectrophotometer 754, Shanghai, China) at a wavelength of 660 nm. Then, the microalgal solutions of different concentrations were transferred to 4 labeled plastic centrifuge tubes. After a low-speed centrifugation at 3000 rpm for 15 min, to each bottle, 50 mL was transferred at a time, for a total of 5 transfers, for a total of 250 mL of algal liquid. The microalgal cells, together with the plastic centrifuge tubes, were dried in a freeze-dryer. After freeze-drying, the plastic centrifuge tubes with the dried algal cells were weighed, and the mass of the empty centrifuge tubes recorded was subtracted to obtain the dry weight of the microalgae corresponding to the absorbance. Since each bottle of centrifuged microalgal solution was 250 mL, the relationship curve between microalgae concentration and OD660 could be deduced and the density of the microalgae with respect to OD660 could be obtained through fitting, as shown in Figure S1.

2.1.3. Selection of Chlorella Concentration

The algae density of *Chlorella vulgaris* showed a good linear relationship with the algae solution at OD660, where R^2 was 0.9999, and the absorbance of the diluted *Chlorella* was chosen to be 0.743 in this experiment.

2.2. Adsorption of Cu(II), Cd(II), and Zn(II) by Chlorella vulgaris

2.2.1. pH and Initial Concentration

Van Hille et al. demonstrated that metal ions react with hydroxide to generate a precipitate at pH values higher than 8.0 [28]. Therefore, the initial pH range was set to 2.0–8.0 for this experiment. Different concentrations of Cu ($CuSO_4 \cdot 5H_2O$), Cd ($CdCl_2$), and Zn ($ZnCl_2$) were added to the microalgal solution with varying initial concentrations (Cu: 0.2, 0.4, 0.8, 1.0, 2 mg/L; Cd: 4, 8, 12, 16, 20 mg/L; Zn: 5, 10, 15, 20, 25 mg/L), which were placed in an orbital oscillatory culture on a thermostatic oscillator at 30 °C and 160 rpm. After 24 h of cultivation, the supernatant was collected after centrifuging at 3000 rpm for 15 min using a low-speed centrifuge. The supernatant was then filtered through a 0.45 μm filter into a centrifuge tube. The concentrations of heavy metals in the supernatant were determined using ICP-OES. Each concentration gradient treatment was repeated twice in parallel experiments.

2.2.2. Adsorption Kinetic Experiments

This research aimed to investigate the impact of various variables on the adsorptive capacity of algae. The adsorptive characteristics of three distinct metals in a Chlorella solution are primarily manifested in three aspects: adsorption rate, adsorption mechanism, and adsorption process. Empirical adsorption models, such as the pseudo-first-order, pseudo-second-order, and intra-particle diffusion kinetic models, were utilized to analyze the experimental adsorption data and clarify the adsorption behavior. A certain amount of 1.0 g/L heavy metal mother liquor was added into the Chlorella solution, and the initial concentrations of the system were 2 mg/L Cu, 12 mg/L Cd, and 5 mg/L Zn. Supernatants were obtained at time intervals of 15, 30, 60, 90, 120, 150, 180, 240, and 300 min, and the ion concentrations were measured using ICP-OES. The calculation Formula (1) for adsorption efficiency is as follows [29]:

$$q = \frac{(C_0 - C_t)V}{M} \tag{1}$$

where C_0 denotes the initial concentration of heavy metal ions (mg/L), C_t represents the concentration of heavy metal ions at time t (mg/L), V signifies the total volume of the adsorption solution (L), M indicates the mass of the adsorbent (g), and q is the adsorption capacity (mg/g).

$$\ln(q_e - q_t) = \ln q_e - k_1 t \tag{2}$$

$$\frac{t}{q_t} = \frac{1}{k_2 {q_e}^2} + \frac{t}{q_e} \tag{3}$$

$$q_t = k_f t^{\frac{1}{2}} + C \tag{4}$$

The three equations above represent the pseudo-first-order (2), pseudo-second-order (3), and intra-particle diffusion kinetic models (4) [30]. In the equations, the variables t, q_t, and q_e denote the adsorption time (min), the heavy metal ion adsorption capacity (mg/g), and the metal ion adsorption capacity at equilibrium (mg/g). The adsorption rate constants k_1 (min^{-1}), k_2 (g/mg/min), and k_f correspond to the pseudo-first-order, pseudo-second-order, and intra-particle diffusion kinetics, respectively.

2.2.3. Adsorption Isothermal Experiments

To attain the maximal adsorption capacity for the three heavy metals in the microalgal solution system, the Langmuir (5) and Freundlich (6) models were utilized to analyze the adsorption data. A certain amount of 1.0 g/L heavy metal mother liquor was added to the

system to form different initial concentrations: Cu: 0.5, 5, 10, 15, 20, 40, 50, 60, 100 mg/L; Cd: 5, 15, 20, 30, 55 mg/L; Zn: 5, 15, 20, 30, 50, 70, 95 mg/L:

$$q_e = \frac{q_m K_L C_e}{1 + K_L C_e} \tag{5}$$

$$q_t = k_f t^{\frac{1}{2}} + C \tag{6}$$

In this equation, C_e denotes the ion concentration at equilibrium (mg/L), q_m signifies the maximal ion adsorption capacity (mg/g) [31], the Freundlich empirical parameter is $1/n$, the Langmuir constant is K_L, and the Freundlich constant is K_f [32].

2.2.4. Determination of Antioxidant Activity

Using the GSH test kit, the concentration of GSH in the microalgal system was quantified before and after the adsorption process. The GSH content reveals the mechanism of GSH in the detoxification and enhancement of heavy metal adsorption capacity of Chlorella, which in turn provides a scientific basis and technical support for the treatment of heavy metal pollution in water bodies.

2.2.5. Determination of Intracellular and Extracellular Heavy Metals

After being subjected to varying pH treatments and initial concentrations of heavy metal ions, Chlorella was dried on 0.45 μm organic filter paper and subsequently filtered before being put into a 20 mL centrifuge tube. The centrifuge tube was filled with 0.2 mol/L nitric acid for three elutions. Nitric acid (0.2 mol/L, Xilong Scientific, Shantou, China) was added to the centrifuge tube for elution (3 times). Each time, 5 mL of nitric acid was added and eluted at 3000 rpm for 30 min. The eluate was collected, transferred to a digestion tube, and digested with digestion solution (nitric acid:sulfuric acid = 3:1) for 2 h. When the volume was constant, the ion concentration in the digestion solution was detected by ICP-OES and the amount of extracellular adsorption was calculated. After the elution process was completed, the algal bodies were retained and digested with nitric acid:perchloric acid (1:1). The specific digestion method was as follows: a total of 9 mL of acid was added, placed in the digestion tubes, digested at 60 °C for 30 min, then heated at 120 °C for 30 min. After cooling to room temperature, 1.2 mL of hydrogen peroxide was added to each tube and digested for 15 min at 120 °C. Finally, the solution was transferred to a 100 mL volumetric flask, the concentration was detected by ICP-OES to determine the digestive concentration, and the amount adsorbed in the cells was calculated.

2.3. Characterization Measurements

2.3.1. XPS Measurements (Thermo Scientific ESCALAB Xi+, Waltham, MA, USA) and XRD Measurements (Bruker D8 Advance, Berlin, Germany)

Chlorella before and after adsorption was washed three times with 0.1 M, pH 7.0 phosphate buffer (PBS buffer), and then, the samples were placed in a freeze-dryer (HORDE-ELECTRIC-HD-LG, Weifang, China) for 24 h. The freeze-dried samples were ground in a 70 μm disposable cell sieve and used in the machine for testing.

2.3.2. SEM-EDX (Zeiss Sigma300, Oberkochen, Germany) and TEM-EDX (Thermo Scientific Talos F200X, Waltham, MA, USA)

Chlorella before and after adsorption was rinsed three times with PBS buffer, fixed with 2.5% glutaraldehyde in the dark for 12 h, poured off the fixative, and rinsed with PBS buffer three times for 15 min each time; the sample was fixed with 1% osmium acid solution for 1–2 h; the osmium acid waste was carefully removed, and the sample was rinsed with PBS buffer three times, 15 min each time; and the sample was dehydrated with gradient concentrations (including 30%, 50%, 70%, 80%, 90%, and 95% concentrations) of ethanol solution for 15 min each. The samples were then treated twice with 100% ethanol for 20 min each time. Finally, the samples were treated with a mixture of ethanol and isoamyl

acetate (v/v = 1/1) for 30 min and then treated with pure isoamyl acetate for 1 h or left overnight. At the critical point, the samples were dried, coated, and observed.

2.3.3. FTIR Measurement (Thermo Scientific Nicolet iS20, Waltham, MA, USA)

The samples were washed three times with PBS buffer, freeze-dried, and ground in a 70 µm disposable cell sieve. The dried 1.0 mg of sample was mixed with 100 mg of KBr and ground thoroughly in an agate mortar. The tablets were then tested by pressing them in the scanning wavelength range of 400–4000 cm^{-1}.

3. Results and Discussions

3.1. Adsorption Experiments

3.1.1. Influence of pH on the Adsorption of Cu(II), Cd(II), and Zn(II)

Due to the speciation of metal ions in the solution and the protonation of functional groups on the adsorbent [33], pH plays a pivotal role in determining the overall stability of microalgal cells. The metabolic activity of microalgae is also highly correlated with pH [34]. The adsorption of heavy metal ions by microorganisms varies significantly with pH levels. Figure 1 illustrates the impact of varying pH conditions on the uptake of Cu(II), Cd(II), and Zn(II) by *Chlorella vulgaris*. *Chlorella vulgaris*'s adsorption efficiency for Cu(II), Cd(II), and Zn(II) progressively rises with increasing pH. The adsorption efficiency of Cu(II) and Cd(II) is relatively poor at pH 2–4, around 40%. In contrast, the adsorption efficiency of Zn(II) is relatively poor at pH < 7, and the adsorption efficiency is around 30%. In an extremely acidic environment, competition for adsorption sites on the adsorbent surface may occur between heavy metal ions and H^+ ions. More adsorption sites become available as the pH rises because OH^- in the solution neutralizes H^+. *Chlorella vulgaris*'s adsorption capacity is increased because the functional groups on its surface are additionally ionized into anions. It gives them an advantage when interacting with the metal cations in the solution [29,35]. It is also likely that the cell membrane's tolerance and permeability are impacted by the solution's low pH, leading to poor cell accumulation, i.e., poor adsorption performance [36].

The results indicate that in extremely acidic conditions (pH 2.0), Chlorella has the lowest efficiency in adsorbing heavy metal ions. This is because extreme acidic conditions can lead to the death of *Chlorella vulgaris*, resulting in decreased adsorption efficiency. The highest adsorption efficiency of *Chlorella vulgaris* for Cu(II), Cd(II), and Zn(II) occurs at pH 7, followed by pH 8, indicating that neutral to slightly alkaline conditions are more favorable for the adsorption of *Chlorella vulgaris*. According to Joo et al. [37], *Chlorella vulgaris* cells' specific surface area grew by 19 times and their ability to adsorb heavy metals increased by 2.4–4.1 times following treatment with sodium hydroxide. In the adsorption process, the rise in extracellular polymeric substances (EPSs) can also be significant [38]. Li et al. [39] found that compared with microbial cells containing extracellular polymers, microbial cells without extracellular polymeric substances have a better adsorption performance for heavy metal ions such as Cu(II), Ni(II), Cd(II), and Zn(II) in aqueous solutions. This suggests that EPS is crucial to the adsorption of heavy metals.

3.1.2. Impact of Varied Initial Concentrations of Cu(II), Cd(II), and Zn(II) on Adsorption

The efficiency of the adsorption process is influenced by the concentration of heavy metal ions in the solution, as it can modify the permeability of cellular membranes and the resistance mechanisms of microorganisms [40]. Figure 2a–c illustrate the adsorption capacity of microalgae for Cu(II), Cd(II), and Zn(II) at different initial ion concentrations under the condition of highest adsorption efficiency at pH = 7. For Cu(II) at concentrations ranging between 0.2 and 2.0 mg/L, microalgae demonstrate excellent adsorption capacity, remaining above 90%, which reaches the highest of 93.63% at the 2.0 mg/L concentration. For Cd(II) at concentrations of less than 12.0 mg/L, the adsorption capacity of Chlorella increases with concentration but decreases when the concentration exceeds 12.0 mg/L. This could be the result of Cd ions interacting with the cells' intrinsic structure, enhancing

the adsorption capability by expanding the adsorption sites. The adsorption capacity of Chlorella is highest at 12.0 mg/L, reaching 73.45%. For Zn(II) at concentrations ranging between 5 and 20 mg/L, the adsorption capacity decreases with increasing concentration, reaching the best adsorption capacity of 85.41% at 5.0 mg/L.

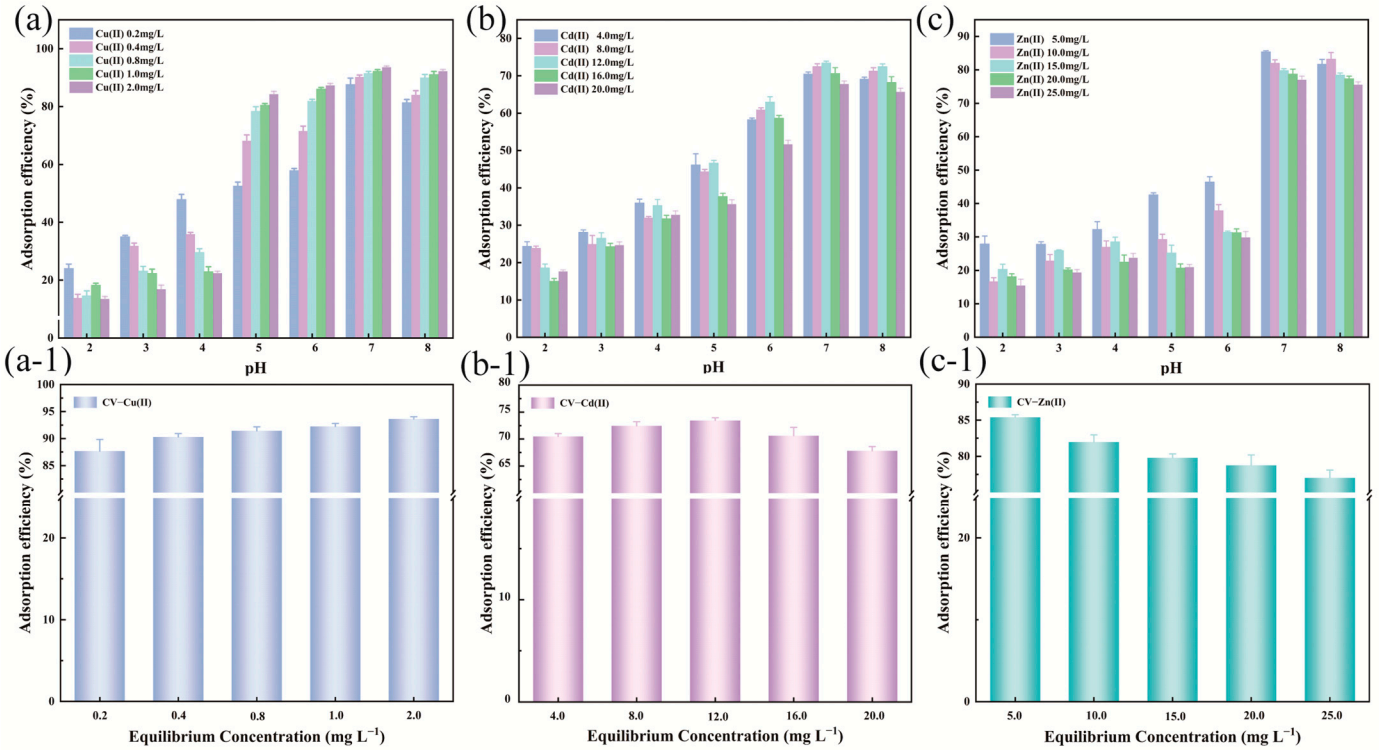

Figure 1. Adsorption capacities of Cu(II) (**a**), Cd(II) (**b**), and Zn(II) (**c**) at different pH values (2.0–8.0) and initial concentrations (Cu(II): 0.2–2.0 mg/L, Cd(II): 4.0–20 mg/L, Zn(II): 5.0–25.0 mg/L), under the experimental conditions of 30 °C and 160 rpm for 24 h. Additionally, the adsorption capacities of Cu(II) (**a-1**), Cd(II) (**b-1**), and Zn(II) (**c-1**) at pH 7 were also evaluated.

3.1.3. Intracellular Adsorption and Extracellular Adsorption

The summarized results indicate that microalgae can effectively remove Cu(II), Cd(II), and Zn(II); however, the adsorption mechanism remains unclear. Therefore, the adsorption of Cu, Cd, and Zn ions in the extracellular and intracellular spaces was studied through analysis and elimination experiments, and the adsorption results are shown in Figure 2a–c. Notably, the extracellular heavy metal content is significantly higher than the intracellular content across various pH gradients and concentration ranges. Specifically, at pH 7, the extracellular content of 2.0 mg/L Cu, 12.0 mg/L Cd, and 4.0 mg/L Zn is 7.65, 22.45, and 13.70 mg/g, respectively. At this time, the intracellular content was 1.40, 2.69 and 3.10 mg/g, respectively. It is easy to conclude that the adsorption of these three ions by microalgae mainly occurs in the extracellular space. In conclusion, microalgae mostly adsorb Cu(II), Cd(II), and Zn(II) through extracellular attachment points, with only a few heavy metal ions entering intracellular adsorption.

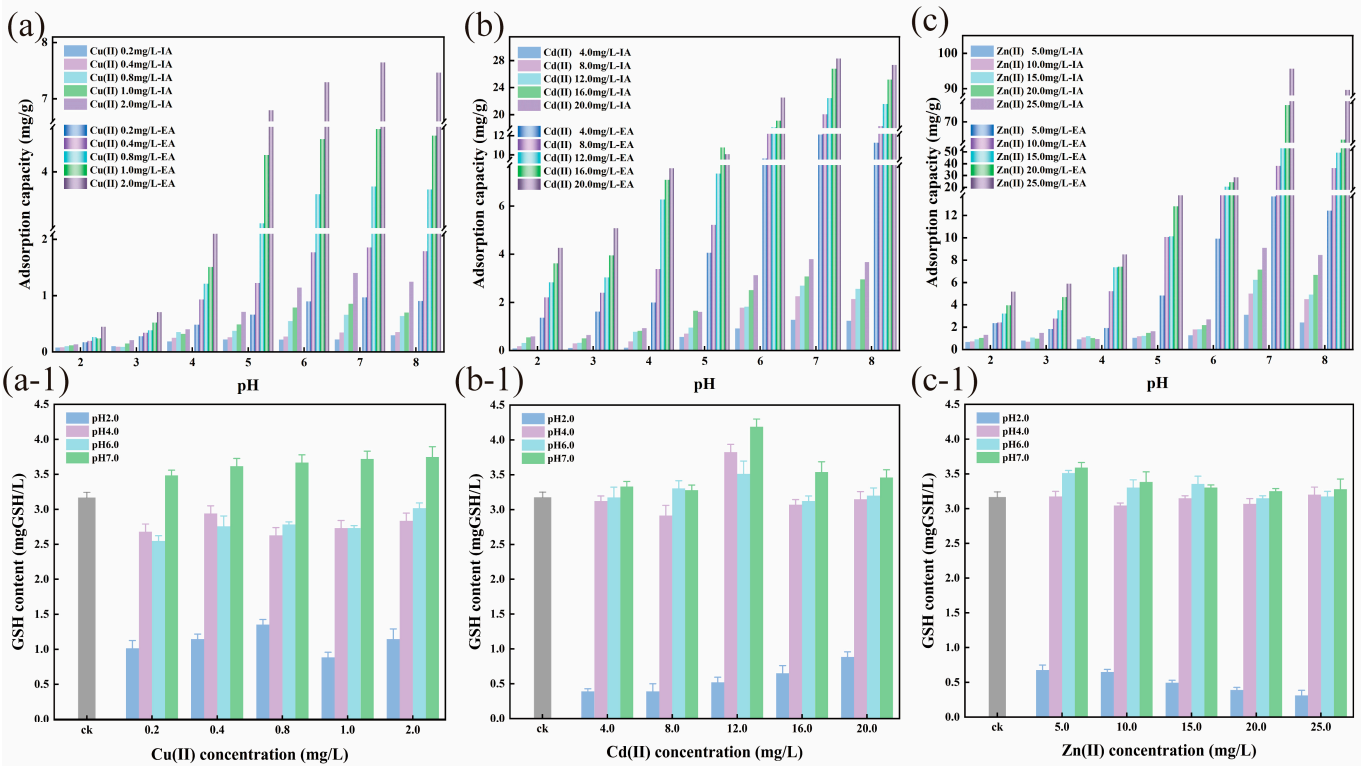

Figure 2. The adsorption capacities of Cu(II) (**a**), Cd(II) (**b**), and Zn(II) (**c**) inside and outside of Chlorella cells at different pH values (2.0–8.0) and initial concentrations (Cu(II): 0.2–2.0 mg/L, Cd(II): 4.0–20 mg/L, Zn(II): 5.0–25.0 mg/L) under the experimental conditions of 30 °C, 160 rpm, and 24 h of adsorption. Additionally, the changes in GSH content before and after adsorption of Cu(II) (**a-1**), Cd(II) (**b-1**), and Zn(II) (**c-1**) were studied.

3.1.4. Changes in Glutathione Content of *Chlorella vulgaris*

Glutathione is a low redox potential tripeptide made up of cysteine, glycine, and glutamic acid. It functions inside the cell as a detoxifier and chelating agent for unbound heavy metal ions. Because of its powerful attraction to ions of heavy metals, it can detoxify the heavy metal ions by forming stable intracellular metal–glutathione complexes. The content of reduced glutathione (GSH) is commonly used to assess the degree of self-repair of algal cells during environmental stress periods [40,41]. To explore the alterations in the oxidation system of the microalgae subsequent to heavy metal binding, the GSH content of the microalgae was monitored before and after 24 h of adsorbing Cu(II), Cd(II), and Zn(II). The results are shown in Figure 3. It can be observed that under extremely acidic conditions (pH = 2), the GSH content after adsorption is much lower than that before adsorption, reflecting the severe damage to the cells. This finding further proves the phenomenon of microalgal death under the unfavorable environment of extreme acidity combined with heavy metal stress. In weakly acidic and neutral environments, the GSH content of the microalgae exhibits distinct trends after adsorbing different heavy metals. Specifically, for Cu adsorption, the GSH content and the initial concentration have a positive correlation. In the case of Cd adsorption, the GSH content initially rises with concentration, reaching its peak at 12 mg/L, and then declines. Conversely, the GSH content after adsorbing Zn shows a negative correlation with concentration. Furthermore, after adsorption in weakly acidic environments, the GSH content decreases compared to pre-adsorption, while under the optimal adsorption conditions (pH = 7), the GSH content after adsorption surpasses the pre-adsorption levels, indicating that the microalgae itself can produce a higher content of GSH to resist the damage of external heavy metal ions to microalgal cells. Additionally, the better the adsorption efficiency, the higher the GSH content, which is consistent with the results of the effects of different initial Cu(II), Cd(II), and Zn(II) concentrations on

adsorption and the effects of pH on Cu(II), Cd(II), and Zn(II) adsorption. These results suggest that enhancing the biosynthesis of intracellular glutathione can effectively alleviate the toxic response to Cu(II), Cd(II), and Zn(II)-induced ecotoxicity; this could be one of the processes by which heavy metals are changed and detoxified in microalgae [42,43].

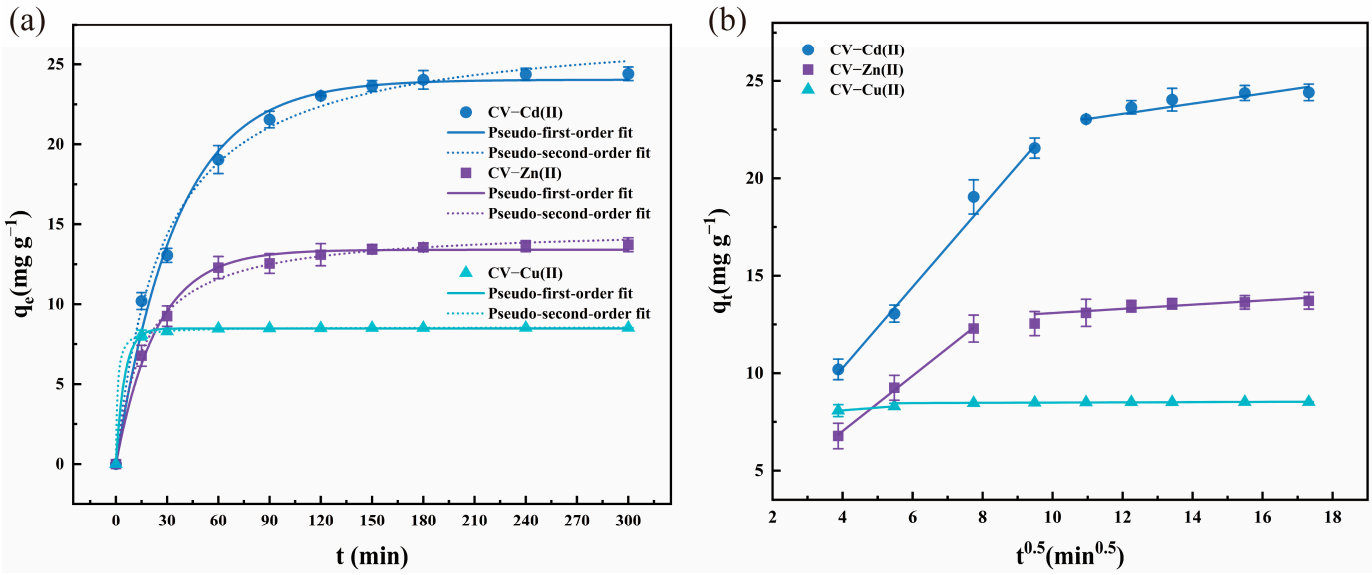

Figure 3. The adsorption of 2 mg/L Cu(II), 12.0 mg/L Cd(II), and 5.0 mg/L Zn(II) by microalgae at pH 7.0, 30 °C, and 160 rpm following the pseudo-first-order and pseudo-second-order kinetics models (**a**), and the adsorption of heavy metals following the intra-particle diffusion kinetics model within the microalgae (**b**).

3.1.5. Dynamics of Adsorption of Cu(II), Cd(II), and Zn(II) by *Chlorella vulgaris*

The adsorptive behavior of *Chlorella vulgaris* towards Cu(II), Cd(II), and Zn(II) was examined through the application of pseudo-first-order, pseudo-second-order, and intra-particle diffusion kinetic models to analyze the organism's adsorption kinetics. The experimental conclusions are shown in Figure 4a and Table S2. The pseudo-second-order kinetic equation for *Chlorella vulgaris*'s heavy metal adsorption (Cd(II): 0.9941; Zn(II): 0.9956; Cu(II): 0.9999) shows R^2 values higher than those of the pseudo-first-order kinetic equation (Cd(II): 0.9915; Zn(II): 0.9948; Cu(II): 0.9995), as illustrated in Table S2. This implies that the pseudo-second-order kinetic model provides a more accurate representation of the adsorption process of *Chlorella vulgaris*. From Figure 4, it is evident that within the first 90 min, the capacity of *Chlorella vulgaris* to adsorb Cd increases rapidly. Then, it slows down until adsorption equilibrium is reached at 120 min. In contrast, approximately 80% of the Zn ions are bound to Chlorella cells within 45 min, with slight increases in absorption between 45 min and 60 min, after which it reaches adsorption equilibrium. Therefore, 60 min is considered the equilibrium time for the adsorption of Zn ions by *Chlorella vulgaris*. It is noteworthy that the ability of *Chlorella vulgaris* to adsorb Cu rapidly increases within the first 15 min, followed by a slow increase between 15 and 20 min, until adsorption reaches equilibrium. When heavy metal ions are added into the Chlorella solution, the adsorption processes of Cd in 90 min, Zn in 45 min, and Cu in 15 min are most likely to be the surface adsorption of cells. This process is passive and rapid and does not involve energy and metabolic adsorption. In practical applications, the advantage of this rapid adsorption is that a small reactor volume can be used. The subsequent gradual increase in adsorption capacity may be due to the intracellular absorption of heavy metal ions, which is an active and slow process that eventually reaches adsorption equilibrium. The aforementioned findings suggest that chemical adsorption is the primary mode of adsorption, with physical adsorption playing a minor role. Similar trends have been observed in many studies on the removal of heavy metals using biological methods [44–46].

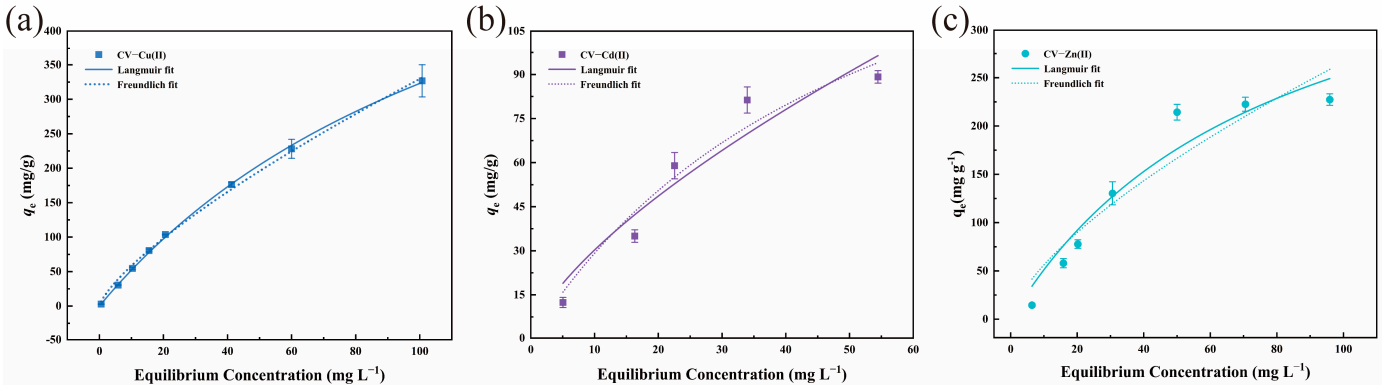

Figure 4. Langmuir and Freundlich models of the adsorption of Cu(II) (**a**), Cd(II) (**b**), and Zn(II) (**c**) by microalgae under the experimental conditions of pH 7.0, 30 °C, 160 rpm, and 0.5–100 mg/L Cu(II), 5–55 mg/L Cd(II), and 5–95 mg/L Zn(II).

In general, several variables, such as surface adsorption, internal diffusion, and external diffusion, regulate the adsorption rate. In this scenario, the hindrance caused by external diffusion resistance can be mitigated through the application of mechanical oscillations, with internal diffusion and surface adsorption governing the adsorption rate [40]. To elucidate the diffusion mechanisms involved in heavy metal adsorption by Chlorella, a kinetic intra-particle diffusion model was used (see Figure 2b and Table S2). The outcomes showed that there are two steps to the adsorption process; $Kf_1 > Kf_2$ suggests that a significant amount of Cu(II), Cd(II), and Zn(II) is adsorbed onto microalgae primarily through external diffusion [47], which is characterized by instantaneous adsorption of the adsorbent and external surface adsorption. As the adsorption sites are occupied in the first stage, the adsorption rate will slow down until it reaches equilibrium, which is the second stage characterized by internal or pore diffusion of the adsorbent particles [48]. Throughout the adsorption process, the second stage emerges as the rate-limiting step. The intercept of the fitted equation, not passing through the origin, suggests that internal diffusion does not solely dictate the rate-limiting step [32,47]. Therefore, Cu(II), Cd(II), and Zn(II) are subject to dual control of internal and external diffusion in the adsorption process of microalgae.

3.1.6. Isothermal Adsorption Modeling of Cu(II), Cd(II), and Zn(II) Adsorption by *Chlorella vulgaris*

Different isotherm models were used to study the metal binding affinity on the surface of adsorbents, as well as the maximum biosorption capacity of various metal ions and adsorbents. The Langmuir model postulates that there is monolayer coverage, that the adsorbate does not migrate on the surface plane, and that each adsorption site has the same adsorption energy [49]. According to the Freundlich model, adsorption occurs on heterogeneous surfaces, with the favorability of adsorption reflected in the value of n [32]. The Langmuir and Freundlich models in Figure 4a–c were used to evaluate the biosorption isotherms of Cu(II), Cd(II), and Zn(II). The constants obtained from the biosorption isotherms are listed in Table S3. A regression analysis of the data shows that LangmuirR_1 is greater than FreundlichR_2. This demonstrates that the attachment of heavy metals to microalgae occurs through monolayer diffusion and that the Langmuir fit is more suitable for the heavy metal adsorption process by microalgae [50]. The Langmuir model calculates the maximal adsorption capacity, which is highest for Cu at 764.547 ± 32.779 mg/g, Zn at 453.193 ± 129.291 mg/g, and Cd at 187.972 ± 65.548 mg/g. Related studies have also shown that the seaweed Sargassum fusiforme and the microalgae *Chlorella vulgaris* follow the Langmuir model, which indicates that adsorption occurs through specific homogeneous sites present in the adsorbent structure, and each of these sites can adsorb a row of molecules. Moreover, it is noteworthy that there is no alteration observed at the initial adsorption site during the early stages of molecule entry. This suggests that the adsorp-

tion process unfolds in a monolayer formation, conforming to a uniform arrangement of adsorbed molecules [51,52].

3.2. Chlorella Morphological Analysis

3.2.1. XRD Analysis of *Chlorella vulgaris*

To determine the form in which heavy metals exist on cell surfaces after the adsorption of Cu(II), Cd(II), and Zn(II) by microalgae, the surface crystal distribution and composition of the microalgae were analyzed using XRD before and after the adsorption process. These findings are displayed in Figure 5a–c. It is evident that NaCl, FeS_2, and C24H32O8 are the primary crystal components on the cell surface before the adsorption of heavy metals. After the adsorption of Cu(II), Cu_2S and CuS_2 are detected by XRD, indicating a reduction phenomenon on the surface of the microalgae during the adsorption of divalent copper, resulting in the reduction of the original divalent copper ions to monovalent copper ions. This is consistent with the results of the high-resolution XPS spectrum of Cu 2p (a-4). However, Cd(II) and Zn(II) do not undergo a valence state transition during the adsorption process, and the presence of CdS and $ZnSO_4$ is detected. This finding aligns with the outcomes from the high-resolution XPS analysis of Cd 3d (b-4) and Zn 2p (c-4) spectra.

3.2.2. XPS Analysis of *Chlorella vulgaris*

At 10 nm in depth, XPS is a practical tool for analyzing the functional and elemental makeup of the surface of microalgal cells. It offers data on electron binding energy and surface chemistry, making it possible to determine the chemical state and elemental makeup of surface constituents [53]. The microalgae were subjected to XPS spectroscopic examination both before and after adsorbing heavy metal ions to gain additional insight into their adsorption mechanism. The conclusions are shown in Figure 5. From the figure, before adsorption, the main elements on the microalgae surface are C, O, and N, and the S signal is weak. After adsorption, distinct characteristic signals of Cu 2p, Cd 3d, and Zn 2p are observed on the microalgae cell surface, indicating the successful binding and adsorption of Cu(II), Cd(II), and Zn(II) to the surface active sites of the algae.

From the high-resolution C 1s spectrum (Figure 5(a-1–c-1,e)), three peaks can be observed in the microcystis. The C-C and C-H bonds (284.8 eV), which make up the carbon skeleton, are represented by the first peak. The hydroxyl, ether, and amine are responsible for the second peak, which are C-O and C-N bonds (285.42 eV) connected to only one oxygen or nitrogen. Finally, the third region corresponds to a carboxyl or ester functional group, i.e., O=C-OH or O=C-OR (288.20 eV)) [32,54]. The results indicate that there is a small deviation in the binding energies of microcystins after adsorbing Cu(II), Cd(II), and Zn(II), which is consistent with the pre-adsorption state. After adsorbing Cu(II), the proportion of C-C and C-H bonds decreases from 35.38% to 33.31%, while the proportion of O=C-OH increases from 6.78% to 7.99%. After adsorbing Cd(II) and Zn(II), the proportion of C-C and C-H bonds increases to 37.22% and 35.66%, respectively, while the proportion of O=C-OH decreases to 6.47% and 4.85%, respectively. In the process of adsorbing Cu(II) and Zn(II), there is a noticeable increase in the prevalence of C-O and C-N bonds, with their proportions rising from 57.84% to 58.70% and 59.49%, respectively. while it decreases to 56.31% after adsorbing Cd(II). This indicates the formation of additional C-O, C-N, and O=C-OH groups in microcystins during Cu(II) adsorption, and additional C-C, C-H groups during Cd(II) adsorption. Furthermore, the adsorption of Zn(II) results in the inclusion of additional C-C, C-H, C-O, and C-N groups. These newly formed groups play a crucial role in improving the efficiency of the adsorption process. Additionally, high-resolution spectra of Cu 2p, Cd 3d, and Zn 2p showed that, upon adsorption, the valence states of Cd(II) and Zn(II) remained unchanged, while Cu(II) underwent a shift in valence state that resulted in the production of Cu(I). This implies that carboxyl or ester functional groups on the cell surface are crucial for Chlorella's ability to adsorb heavy metals.

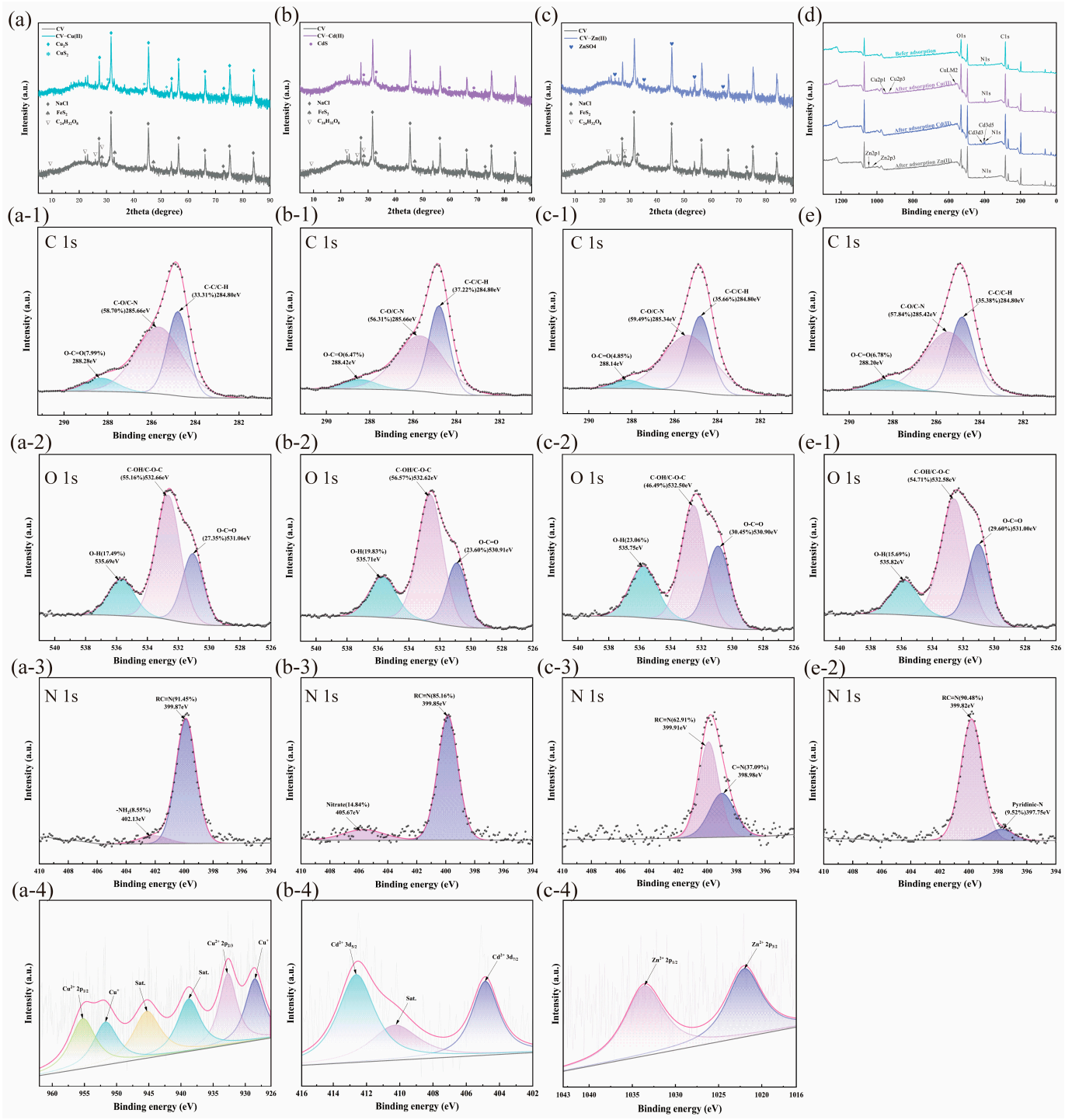

Figure 5. XRD of microalgae before and after adsorption of 2 mg/L Cu(II) (**a**), 12.0 mg/L Cd(II) (**b**), and 4.0 mg/L Zn(II) (**c**) under the experimental conditions of adsorption at pH 7.0, 30 °C, and 160 rpm for 24 h; XPS survey spectra after 24 h adsorption of 2 mg/L Cu(II), 12.0 mg/L Cd(II), and 4.0 mg/L Zn(II) (**d**); high-resolution XPS spectra of C 1s: (**e**) before adsorption and (**a-1**–**c-1**) after adsorption of Cu(II), Cd(II), and Zn(II), respectively; high-resolution XPS spectra of O 1s: (**e-1**) before adsorption and (**a-2**–**c-2**) after adsorption of Cu(II), Cd(II), and Zn(II), respectively; high-resolution XPS spectra of N 1s: (**e-2**) before adsorption and (**a-3**–**c-3**) after adsorption of Cu(II), Cd(II), and Zn(II), respectively; high-resolution XPS spectra of Cu 2p (**a-4**), Cd 3d (**b-4**), and Zn 2p (**c-4**) for microalgae.

High-resolution O 1s XPS spectra (Figure 5(e,a-2–c-2,e-1)) exhibited three peaks in the O 1s spectrum in the coexisting system. The first peak corresponds to O-C=O (531.00 eV),

the second peak is attributed to C-OH/C-O-C (532.58 eV), and the third peak corresponds to O-H (535.82 eV) [55]. Similar to the results of C 1s, there is minimal deviation in the binding energy before and after adsorption, with O-C=O groups decreasing from 29.60% to 27.35% and 23.60% after adsorbing Cu(II) and Cd(II), respectively. Following Cu(II) and Cd(II) adsorption, the percentage of C-OH/C-O-C groups rises from 54.71% to 55.16% and 56.57%, respectively, while the -OH group increases to 30.45% and the C=O/C-O group decreases to 46.49% after the adsorption of Zn(II). Furthermore, after adsorbing these three heavy metals, the proportion of O-H groups increases to 17.49%, 19.83%, and 23.06%, respectively. It is evident that the oxygen-containing groups exhibit similar behavior when adsorbing Cu(II) and Cd(II) but differ when adsorbing Zn(II). This may be attributed to the different functional groups binding the metal ions, leading to different complexation products. XRD indicated that the products of Cu(II) and Cd(II) adsorption are sulfides, while the product of Zn(II) adsorption is a sulfate compound. Related studies also suggested that oxygen has a high electronegativity, and some oxygen-containing functional groups (such as COOH, O-H, etc.) with partial negative charges on the oxygen atoms able to adsorb heavy metals through ion exchange [56].

From the high-resolution N 1s spectrum (Figure 5(a-3–c-3,e-2)), it can be observed that before the adsorption of microalgae, the N 1s spectrum has two peaks of pyridinic-N (397.75 eV) and RC≡N (399.82 eV) [57,58]. The binding energy of the -NH and -NH_2 groups remains relatively unchanged from the pre-adsorption levels following the adsorption. Meanwhile, the proportion of RC≡N increases from 90.48% to 91.45% after adsorbing Cu(II), decreases to 85.16% after adsorbing Cd(II), and decreases to 62.91% after adsorbing Zn(II), making a reduction of 27.57%. Furthermore, when microalgae adsorb these three heavy metal ions, the binding energy at 397.75 eV undergoes significant migration, possibly because the protonated -NH_3^+ groups on the surface of the microalgae coordinate with the metal ions, resulting in the changes in relevant bond energies [40], or because the heavy metal ions bind with the polysaccharides and proteins of the EPS on the cell surface, causing a shift in binding energy [58]. Specifically, during the adsorption of Cu(II), the binding energy migrates from 397.75 eV to 402.13 eV, and the functional group is converted to -NH_2 [59], leading to a decrease in its proportion from 9.52% to 8.55%. In the process of treating Cd(II), the binding energy migrates to 405.27 eV [60], and the functional group is converted to nitrate, leading to an increase in its proportion to 14.84%. During the adsorption of Zn(II), the binding energy migrates to 398.98 eV, and the functional group is converted to C=N [54], leading to an increase in its proportion to 37.09%.

The study's XPS data revealed that the surface of the Chlorella cell wall contains a variety of characteristic groups, such as carboxyl, amino, aldehyde, and ether groups. These groups were involved in interactions with Cu(II), Cd(II), and Zn(II) during the adsorption process by Chlorella. The binding of heavy metals by these functional groups contributes to their removal. Zhao et al. [61] discovered that the fungus Geotrichum sp. dwc-1 had functional groups like amide and carboxylic acid that are crucial for binding heavy metals in XPS. Wang et al. [62] discovered through XPS that functional groups in modified microalgae Chlorella, such as -SH and -OS_3O-, can also bind to Hg(II) and adsorb toxic mercury ions under low sulfur conditions in the environment.

3.2.3. FTIR Analysis of *Chlorella vulgaris*

The FTIR spectra of microalgae with *Chlorella vulgaris*, both in the presence and absence of Cu(II), Cd(II), and Zn(II), are depicted in Figure 6. The broad peaks observed in the range of 3430–2927 cm^{-1} correspond to the characteristic functional groups of hydroxyl, phenol, alcohol, and carboxyl. The peak at 3395 cm^{-1} is due to the presence of -OH. The peaks within the range of 1656–1542 cm^{-1} are identified as absorption peaks, denoting the amide I and II vibrations of the C-N groups associated with the peptides on the cellular surface, as indicated by the peaks at 1656 and 1542 cm^{-1} [63], and the functional groups in this range make a significant contribution to the effective removal of metal ions. The absorption peak at 1451 cm^{-1} is caused by the bending vibrations of the C-H aliphatic group. Furthermore,

the peak at 1244 cm^{-1} is attributed to the phosphodiester bonds found in phospholipids and nucleic acids [64]. The asymmetric stretching vibration of C-O-C, which is indicative of ester bonds in proteins like hemoglobin, is observed at 1157 cm^{-1}. The peak at 1076 cm^{-1} represents the stretching vibration of the C-OH bond in carboxyl groups, which are prevalent in lipids, proteins, and carbohydrates (refer to Table S4). Additionally, the peak at 931–860 cm^{-1} corresponds to the region where olefins (=C-H) are present.

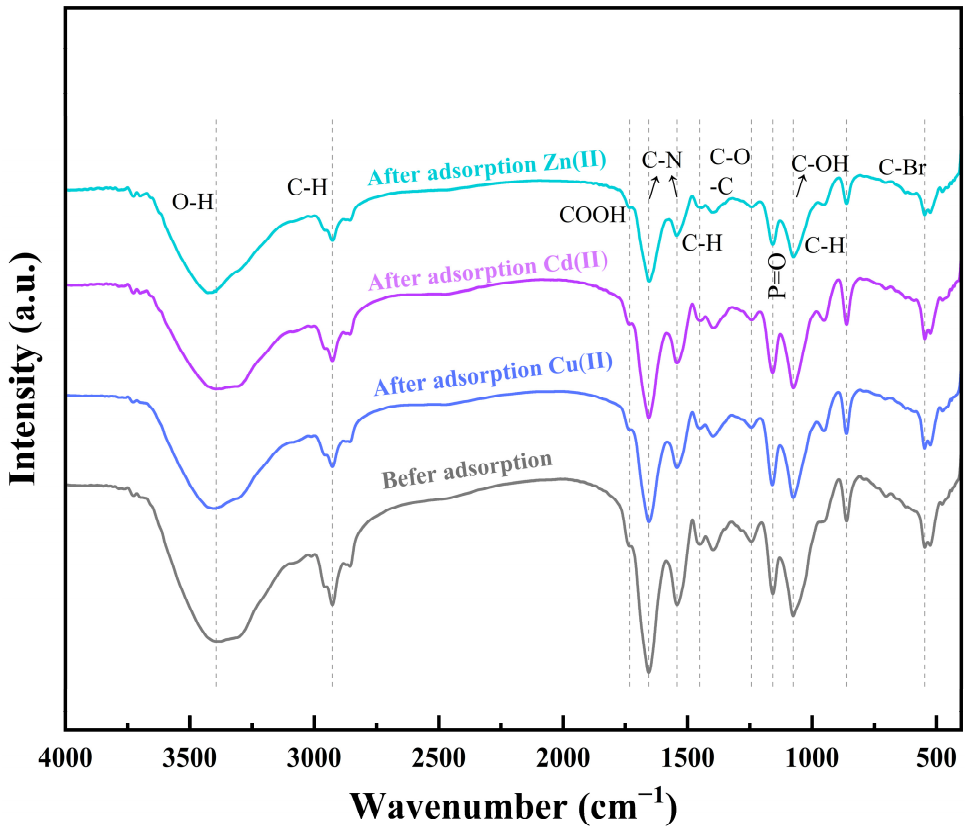

Figure 6. FTIR peaks before and after adsorption of Chlorella at concentrations of 2 mg/L Cu(II), 12 mg/L Cd(II), and 5 mg/L Zn(II) at pH 7.0 and 30 °C.

Numerous studies have demonstrated that cells' surfaces are adorned with negatively charged functional groups, including COOH, O-H, and P=O, which can undergo ion exchange with heavy metal ions, constituting a mechanism for biological adsorption [65]. Bifunctional structures with characteristic groups such as C-N, P=O, and O-H are also very effective at chelating heavy metal ions, in addition to negatively charged functional groups. From the graphs, it can be seen that the peaks before and after adsorption changed significantly around 1732, 1656, 1542, 1244, 1157, and 1075 cm-1. These changes correspond to the vibrational frequencies of COOH, C-N, P=O, C-O-C, and C-OH functional groups, respectively. This finding suggests that Cu(II), Cd(II), and Zn(II) can bind to specific functional groups on the microalgae's surface to facilitate adsorption. Consequently, this validates the involvement of diverse functional groups observed in XPS with heavy metal ions during the adsorption process.

3.2.4. Morphometric Analysis of *Chlorella vulgaris* Using SEM-EDS

The morphological characteristics of microbial cells can be examined using SEM. This technique allows for the analysis of alterations in the surface morphology of cells following the adsorption of heavy metal ions. The surface properties of algal biosorbents after adsorbing Cu(II), Cd(II), and Zn(II) were characterized using SEM, and the electron micrographs are shown in Figure 7(a–d,a-1–d-1). It is evident that the microalgae maintain a spherical shape and have folds on the cell surface, providing a good condition for the

fixation of heavy metals. Before adsorption, the surface of microalgae cells is smooth, without any attachment, and the cell structure is intact. After the adsorption of Cu(II), the surface texture of the microalgal cells shows increased roughness, similar to a mesh, and exhibits shrinkage and deformation. In addition, particulate matter is attached to the cell surface. Following the uptake of Zn(II) and Cd(II) by microalgae, different degrees of damage and disintegration of microalgal cells can be observed, as shown in Figure 7. Numerous asymmetric crystal micro-precipitates are seen on the surface of the microalgal cells. The disintegration of cell structures could be attributed to the lysis of the cell wall and membrane induced by heavy metal ions, which disrupts the cellular architecture. The formation of microprecipitates on cell surfaces is a crucial and highly significant mechanism for the biosorption-based removal of heavy metals [66]. Furthermore, Chlorella cell surfaces contain sites for adsorbing heavy metals [67]. The cell wall of microalgae is mainly composed of EPS consisting of polysaccharides, lipids, and proteins, which provide various functional groups. Since these substances contain functional groups with negative charges, they interact with heavy metal cations to form complex compounds, which can help in the adsorption, fixation, and precipitation of metal ions, thereby reducing the toxicity of heavy metals [68]. Wang et al. [62] found that after Chlorella adsorbed Hg(II), the EPS present on the cell surface can form complexes with Hg(II) to produce protruding particles and create metallic minerals bound by Hg(II). Meanwhile, observations by S. Li et al. [69] used SEM to demonstrate that Chlamydomonas reinhardtii forms Pb-containing minerals on its cell surface following the adsorption of Pb(II).

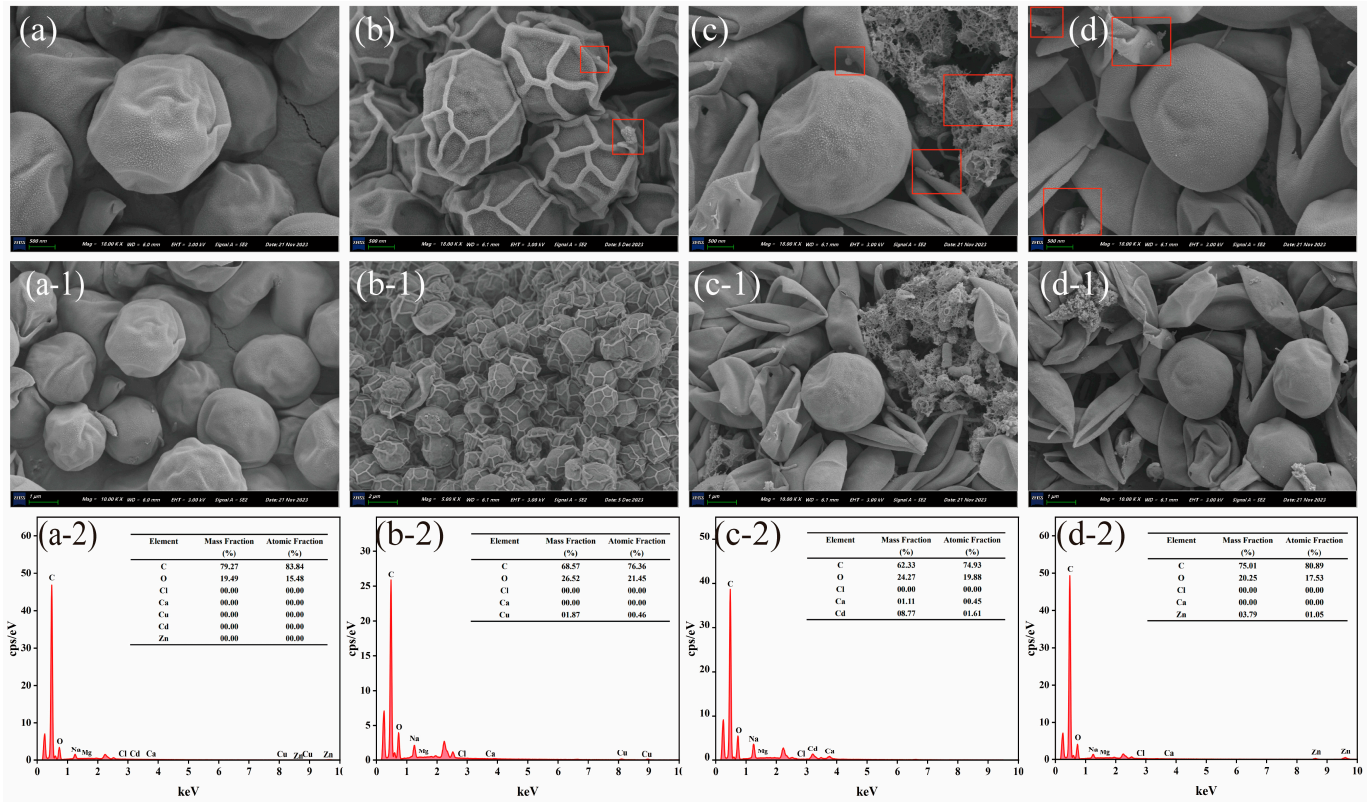

Figure 7. Under the experimental conditions of pH 7.0, 30 °C and 160 rpm adsorption for 24 h, Chlorella adsorbed 2 mg/L Cu(II) (**b**), 12.0 mg/L Cd(II) (**c**), and 4.0 mg/L Zn(II) (**d**) before (**a**) and after SEM at 500 nm magnification. and SEM before (**a-1**) and after adsorption of Cd(II) (**c-1**) and Zn(II) (**d-1**) at 1 μm magnification; SEM after adsorption of Cu(II) (**b-1**) at 2 μm magnification; EDX of Chlorella before (**a-2**) and after adsorption of Cu(II) (**b-2**), Cd(II) (**c-2**), and Zn(II) (**d-2**).

An examination of the distribution of heavy metal elements on the surface of microalgae cells was conducted using EDS, which revealed localized signals of copper, cadmium, and zinc. This observation implies that the algal cell surface has effectively absorbed and

fixed Cu(II), Cd(II), and Zn(II). Furthermore, it was observed that the surface concentrations of Cu, Cd, and Zn on the cells were elevated compared to the intracellular heavy metal contents, indicating that extracellular adsorption exhibits superior adsorptive capabilities. In addition, calcium signals appear on the cell surface after adsorbing Cd(II), which may be due to the formation of secondary minerals containing calcium ions on the surface. There are no chloride signals before and after the adsorption of the three ions, indicating that no chlorinated inorganic compounds are produced after adsorption. Morphological changes in microalgal cells and elemental analysis confirm the bioabsorption of heavy metals on the cell surface.

3.2.5. Morphometric Analysis of *Chlorella vulgaris* Using TEM-EDS

Utilizing TEM, the ultrastructural characteristics of the cells were investigated, and the intracellular distribution of heavy metal ions was determined. The TEM micrographs of the microalgae after adsorbing Cu(II), Cd(II), and Zn(II) are displayed in Figure 8a–d. From the figures, different positions, sizes, and shapes of black spots (indicated by arrows) appear within the adsorbed microalgal cells, possibly due to the accumulation of heavy metals inside the cells. Li et al. [58] also observed using TEM the accumulation of zinc in Chlamydomonas reinhardtii cells to form aggregates after zinc adsorption. Cheng et al. [70] further demonstrated that uranium can enter *Ankistrodsemus* sp. cells through normal metabolic processes and form uranium-containing crystals.

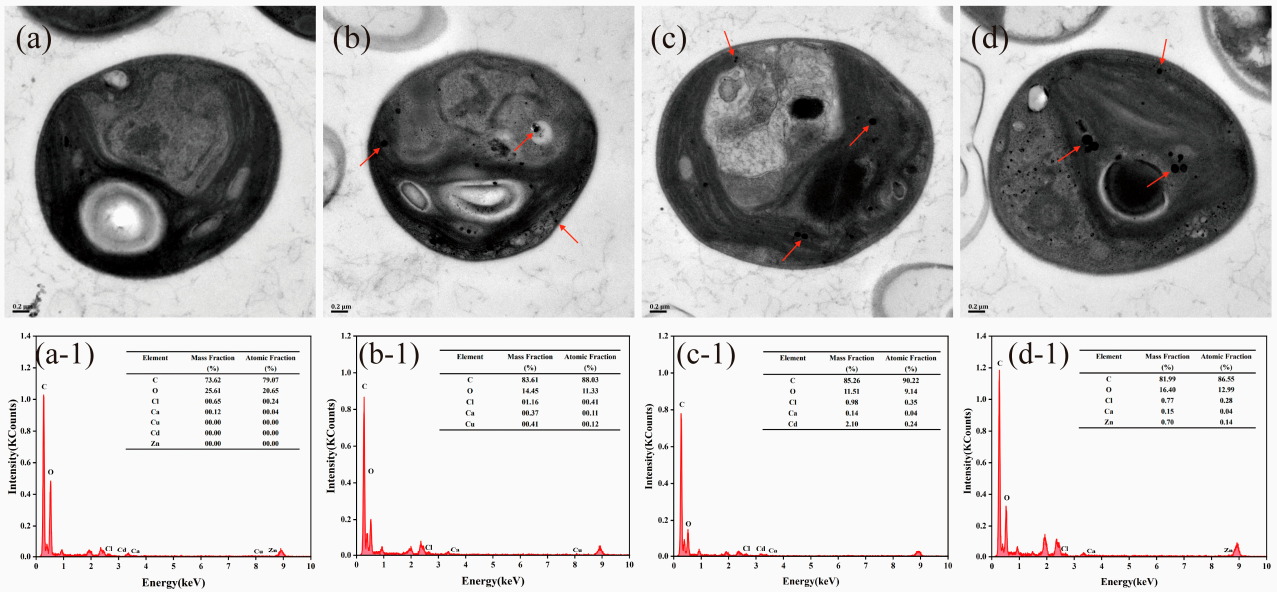

Figure 8. TEM images of Chlorella before (**a**) and after adsorption of 2 mg/L Cu(II) (**b**), 12.0 mg/L Cd(II) (**c**), and 4.0 mg/L Zn(II) (**d**) and EDS of Chlorella before (**a-1**) and after adsorption of Cu(II) (**b-1**), Cd(II) (**c-1**), and Zn(II) (**d-1**) under the experimental conditions of pH 7.0, 30 °C, and 160 rpm for 24 h.

EDS was used to investigate the elemental content of these black dot-like particles in order to further confirm their composition (Figure 8(a-1–d-1)). The figures show that modest indications of copper, cadmium, and zinc appear following the adsorption of Cu(II), Cd(II), and Zn(II) by microalgae, and their relative levels are substantially lower than those outside the cells, proving that Cu(II), Cd(II), and Zn(II) can penetrate the cell wall and cell membrane into the interior of the cells.

4. Conclusions

In this investigation, the adsorption characteristics of copper, cadmium, and zinc within *Chlorella vulgaris* were examined, elucidating the biomineralization and morphological transformation mechanisms of ions. At pH 7.0, with initial concentrations of 2 mg/L Cu(II), 12 mg/L Cd(II), and 12 mg/L Zn(II), *Chlorella vulgaris* exhibited optimal adsorption ef-

ficiency, reaching 93.63%, 73.45%, and 85.41% for Cu(II), Cd(II), and Zn(II), respectively, with adsorption equilibrium time at 20 min, 120 min, 60 min respectively. The adsorption kinetics of Cu(II), Cd(II), and Zn(II) by *Chlorella vulgaris* were primarily governed by pseudo-second-order kinetics and the Langmuir isotherm model. This suggests that the predominant mechanisms are monolayer adsorption and chemisorption. The rate of adsorption is influenced by both intracellular and extracellular diffusion processes, with extracellular adsorption identified as the primary mechanism. There is very little heavy metal ion absorption occurring within the cells. Functional groups had significant roles in the adsorption process and included amino, carboxyl, aldehyde, and ether. However, CdS precipitates, Ca-containing crystals, and $ZnSO_4$ crystals were found on the cellular exterior. Meanwhile, throughout the adsorption process, Cu(II) was reduced to Cu(I), and the generated products included Cu_2S and CuS_2. In the current study of Chlorella, although it has a strong adsorption capacity for heavy metals, when the concentration of heavy metals in the water body exceeds its tolerance level, it may lead to the death of Chlorella. In the future, Chlorella species with higher tolerance and stronger adsorption capacity for heavy metals can be cultivated through genetic engineering or breeding techniques.

Supplementary Materials: The following supporting information can be downloaded at https://www.mdpi.com/article/10.3390/w16131906/s1, Figure S1: Standard curve of chlorella dry weight; Table S1: The compositions of BG11 culture medium; Table S2: The adsorption kinetic model parameters; Table S3: The adsorption isotherm model parameters; Table S4: Peak wavelengths before and after chlorella adsorption of heavy metals.

Author Contributions: Conceptualization, S.L. and M.J.; methodology, M.J.; software, J.W.; validation, M.J., J.W. and X.L.; formal analysis, J.Z.; investigation, X.L.; resources, S.L.; data curation, J.W.; writing—original draft preparation, M.J.; writing—review and editing, S.L.; visualization, M.J.; supervision, S.L.; project administration, J.W.; funding acquisition, S.L. All authors have read and agreed to the published version of the manuscript.

Funding: This research was funded by the Anhui Provincial Natural Science Foundation grant number 2208085QB63 and the National Natural Science Foundation of China grant number 22206003; and the APC was funded by the Scientific Research Foundation of Anhui Universities grant number KJ2021A0442.

Data Availability Statement: The data that support the findings of this study are available on request from the corresponding author, [Liu, S.], upon reasonable request.

Acknowledgments: We appreciate the financial support from the Anhui Provincial Natural Science Foundation (2208085QB63), the Scientific Research Foundation of Anhui Universities (KJ2021A0442), the National Natural Science Foundation of China (22206003).

Conflicts of Interest: The authors declare no conflict of interest.

References

1. Saravanan, A.; Senthil Kumar, P.; Jeevanantham, S.; Karishma, S.; Tajsabreen, B.; Yaashikaa, P.R.; Reshma, B. Effective water/wastewater treatment methodologies for toxic pollutants removal: Processes and applications towards sustainable development. *Chemosphere* **2021**, *280*, 130595. [CrossRef] [PubMed]
2. Hanafiah, Z.M.; Azmi, A.R.; Wan-Mohtar, W.A.A.Q.I.; Olivito, F.; Golemme, G.; Ilham, Z.; Jamaludin, A.A.; Razali, N.; Halim-Lim, S.A.; Wan Mohtar, W.H.M. Water Quality Assessment and Decolourisation of Contaminated Ex-Mining Lake Water Using Bioreactor Dye-Eating Fungus (BioDeF) System: A Real Case Study. *Toxics* **2024**, *12*, 60. [CrossRef] [PubMed]
3. Nabipour, H.; Rohani, S.; Batool, S.; Yusuff, A.S. An overview of the use of water-stable metal-organic frameworks in the removal of cadmium ion. *J. Environ. Chem. Eng.* **2023**, *11*, 109131. [CrossRef]
4. Kumari, M.; Bhattacharya, T. A review on bioaccessibility and the associated health risks due to heavy metal pollution in coal mines: Content and trend analysis. *Environ. Dev.* **2023**, *46*, 100859. [CrossRef]
5. Zhao, K.; Zhao, X.; Gao, T.; Li, X.; Wang, G.; Pan, X.; Wang, J. Dielectrophoresis-assisted removal of Cd and Cu heavy metal ions by using Chlorella microalgae. *Environ. Pollut.* **2023**, *334*, 122110. [CrossRef] [PubMed]
6. Pandey, S.; Kumari, N. Chapter 8—Impact assessment of heavy metal pollution in surface water bodies. In *Metals in Water*; Shukla, S.K., Kumar, S., Madhav, S., Mishra, P.K., Eds.; Elsevier: Amsterdam, The Netherlands, 2023; pp. 129–154.
7. Nriagu, J. Zinc Toxicity in Humans. In *Encyclopedia of Environmental Health*, 2nd ed.; Nriagu, J., Ed.; Elsevier: Oxford, UK, 2019; pp. 500–508.

8. León-Vaz, A.; Romero, L.C.; Gotor, C.; León, R.; Vigara, J. Dataset for proteomic analysis of Chlorella sorokiniana cells under cadmium stress. *Data Brief* **2020**, *33*, 106544. [CrossRef] [PubMed]
9. Galdieri, J.; Adams, C.; Padilla, M.; Stawicki, T.M. The role of calcium, Akt and ERK signaling in cadmium-induced hair cell death. *Mol. Cell. Neurosci.* **2023**, *124*, 103815. [CrossRef]
10. Hernández-Cruz, E.Y.; Amador-Martínez, I.; Aranda-Rivera, A.K.; Cruz-Gregorio, A.; Pedraza Chaverri, J. Renal damage induced by cadmium and its possible therapy by mitochondrial transplantation. *Chem.-Biol. Interact.* **2022**, *361*, 109961. [CrossRef]
11. Luo, H.; Gu, R.; Ouyang, H.; Wang, L.; Shi, S.; Ji, Y.; Bao, B.; Liao, G.; Xu, B. Cadmium exposure induces osteoporosis through cellular senescence, associated with activation of NF-κB pathway and mitochondrial dysfunction. *Environ. Pollut.* **2021**, *290*, 118043. [CrossRef]
12. Song, X.; Liu, B.-F.; Kong, F.; Song, Q.; Ren, N.-Q.; Ren, H.-Y. Simultaneous chromium removal and lipid accumulation by microalgae under acidic and low temperature conditions for promising biodiesel production. *Bioresour. Technol.* **2023**, *370*, 128515. [CrossRef]
13. Badmus, S.O.; Oyehan, T.A.; Saleh, T.A. Enhanced efficiency of polyamide membranes by incorporating cyclodextrin-graphene oxide for water purification. *J. Mol. Liq.* **2021**, *340*, 116991. [CrossRef]
14. Chen, Q.; Yao, Y.; Li, X.; Lu, J.; Zhou, J.; Huang, Z. Comparison of heavy metal removals from aqueous solutions by chemical precipitation and characteristics of precipitates. *J. Water Process Eng.* **2018**, *26*, 289–300. [CrossRef]
15. Torres-Perez, J.; Huang, Y.; Bazargan, A.; Khoshand, A.; McKay, G. Two-stage optimization of Allura direct red dye removal by treated peanut hull waste. *SN Appl. Sci.* **2020**, *2*, 475. [CrossRef]
16. León-Vaz, A.; León, R.; Díaz-Santos, E.; Vigara, J.; Raposo, S. Using agro-industrial wastes for mixotrophic growth and lipids production by the green microalga Chlorella sorokiniana. *New Biotechnol.* **2019**, *51*, 31–38. [CrossRef] [PubMed]
17. Zhao, Y.; Ngo, H.H.; Yu, X. Phytohormone-like small biomolecules for microalgal biotechnology. *Trends Biotechnol.* **2022**, *40*, 1025–1028. [CrossRef] [PubMed]
18. Izadpanah, M.; Gheshlaghi, R.; Mahdavi, M.A.; Elkamel, A. Effect of light spectrum on isolation of microalgae from urban wastewater and growth characteristics of subsequent cultivation of the isolated species. *Algal Res.* **2018**, *29*, 154–158. [CrossRef]
19. Akhtar, N.; Iqbal, M.; Zafar, S.I.; Iqbal, J. Biosorption characteristics of unicellular green alga Chlorella sorokiniana immobilized in loofa sponge for removal of Cr(III). *J. Environ. Sci.* **2008**, *20*, 231–239. [CrossRef] [PubMed]
20. Yoshida, N.; Ikeda, R.; Okuno, T. Identification and characterization of heavy metal-resistant unicellular alga isolated from soil and its potential for phytoremediation. *Bioresour. Technol.* **2006**, *97*, 1843–1849. [CrossRef]
21. Hockaday, J.; Harvey, A.; Velasquez-Orta, S. A comparative analysis of the adsorption kinetics of Cu^{2+} and Cd^{2+} by the microalgae *Chlorella vulgaris* and Scenedesmus obliquus. *Algal Res.* **2022**, *64*, 102710. [CrossRef]
22. Bwapwa, J.K.; Jaiyeola, A.T.; Chetty, R. Bioremediation of acid mine drainage using algae strains: A review. *S. Afr. J. Chem. Eng.* **2017**, *24*, 62–70. [CrossRef]
23. Worms, I.; Simon, D.F.; Hassler, C.S.; Wilkinson, K.J. Bioavailability of trace metals to aquatic microorganisms: Importance of chemical, biological and physical processes on biouptake. *Biochimie* **2006**, *88*, 1721–1731. [CrossRef]
24. Mang, K.C.; Ntushelo, K. Algae-Based Heavy Metal Remediation in Acid Mine Drainage: A Review. *Appl. Ecol. Environ. Res.* **2020**, *18*, 2499–2512. [CrossRef]
25. Brar, K.K.; Etteieb, S.; Magdouli, S.; Calugaru, L.; Brar, S.K. Novel approach for the management of acid mine drainage (AMD) for the recovery of heavy metals along with lipid production by *Chlorella vulgaris*. *J. Environ. Manag.* **2022**, *308*, 114507. [CrossRef]
26. Du, T.; Bogush, A.; Edwards, P.; Stanley, P.; Lombardi, A.T.; Campos, L.C. Bioaccumulation of metals by algae from acid mine drainage: A case study of Frongoch Mine (UK). *Environ. Sci. Pollut. Res. Int.* **2022**, *29*, 32261–32270. [CrossRef]
27. Chojnacka, K.; Chojnacki, A.; Górecka, H. Biosorption of Cr^{3+}, Cd^{2+} and Cu^{2+} ions by blue–green algae Spirulina sp.: Kinetics, equilibrium and the mechanism of the process. *Chemosphere* **2005**, *59*, 75–84. [CrossRef] [PubMed]
28. Van Hille, R.P.; Boshoff, G.A.; Rose, P.D.; Duncan, J.R. A continuous process for the biological treatment of heavy metal contaminated acid mine water. *Resour. Conserv. Recycl.* **1999**, *27*, 157–167. [CrossRef]
29. Karimi, F.; Ayati, A.; Tanhaei, B.; Sanati, A.L.; Afshar, S.; Kardan, A.; Dabirifar, Z.; Karaman, C. Removal of metal ions using a new magnetic chitosan nano-bio-adsorbent; A powerful approach in water treatment. *Environ. Res.* **2022**, *203*, 111753. [CrossRef] [PubMed]
30. Soto-Ramírez, R.; Tavernini, L.; Lobos, M.-G.; Poirrier, P.; Chamy, R. Thermodynamic and kinetic insights into the adsorption mechanism of Cd(II) using *Chlorella vulgaris* cells with coverage modified by culture media engineering. *Algal Res.* **2023**, *74*, 103179. [CrossRef]
31. Dirbaz, M.; Roosta, A. Adsorption, kinetic and thermodynamic studies for the biosorption of cadmium onto microalgae *Parachlorella* sp. *J. Environ. Chem. Eng.* **2018**, *6*, 2302–2309. [CrossRef]
32. Jiang, X.; Yin, X.; Tian, Y.; Zhang, S.; Liu, Y.; Deng, Z.; Lin, Y.; Wang, L. Study on the mechanism of biochar loaded typical microalgae Chlorella removal of cadmium. *Sci. Total Environ.* **2022**, *813*, 152488. [CrossRef]
33. Repo, E.; Warchol, J.K.; Kurniawan, T.A.; Sillanpää, M.E.T. Adsorption of Co(II) and Ni(II) by EDTA- and/or DTPA-modified chitosan: Kinetic and equilibrium modeling. *Chem. Eng. J.* **2010**, *161*, 73–82. [CrossRef]
34. Chu, R.; Li, S.; Yin, Z.; Hu, D.; Zhang, L.; Xiang, M.; Zhu, L. A fungal immobilization technique for efficient harvesting of oleaginous microalgae: Key parameter optimization, mechanism exploration and spent medium recycling. *Sci. Total Environ.* **2021**, *790*, 148174. [CrossRef]

35. Yang, L.; Tan, W.-F.; Mumford, K.; Ding, L.; Lv, J.-W.; Zhang, X.-W.; Wang, H.-Q. Effects of phosphorus-rich sawdust biochar sorption on heavy metals. *Sep. Sci. Technol.* **2018**, *53*, 2704–2716. [CrossRef]
36. Wang, J.; Tian, Q.; Cui, L.; Cheng, J.; Zhou, H.; Peng, A.; Qiu, G.; Shen, L. Effect of extracellular proteins on Cd(II) adsorption in fungus and algae symbiotic system. *J. Environ. Manag.* **2022**, *323*, 116173. [CrossRef]
37. Joo, G.; Lee, W.; Choi, Y. Heavy metal adsorption capacity of powdered *Chlorella vulgaris* biosorbent: Effect of chemical modification and growth media. *Environ. Sci. Pollut. Res.* **2021**, *28*, 25390–25399. [CrossRef] [PubMed]
38. Pagliaccia, B.; Carretti, E.; Severi, M.; Berti, D.; Lubello, C.; Lotti, T. Heavy metal biosorption by Extracellular Polymeric Substances (EPS) recovered from anammox granular sludge. *J. Hazard. Mater.* **2022**, *424*, 126661. [CrossRef] [PubMed]
39. Li, M.; Deng, X.; Sun, W.; Hu, L.; Zhong, H.; He, Z.; Xiong, D. Extracellular polymeric substances of acidophilic microorganisms play a crucial role in heavy metal ions adsorption. *Int. J. Environ. Sci. Technol.* **2022**, *19*, 4857–4868. [CrossRef]
40. Wang, J.; Tian, Q.; Cui, L.; Cheng, J.; Zhou, H.; Zhang, Y.; Peng, A.; Shen, L. Bioimmobilization and transformation of chromium and cadmium in the fungi-microalgae symbiotic system. *J. Hazard. Mater.* **2023**, *445*, 130507. [CrossRef] [PubMed]
41. Wang, H.; Wang, C.; Ge, B.; Zhang, X.; Zhou, C.; Yan, X.; Ruan, R.; Cheng, P. Effect of heavy metals in aquaculture water on the growth of microalgae and their migration mechanism in algae-shellfish system. *Chem. Eng. J.* **2023**, *473*, 145274. [CrossRef]
42. Freeman, J.L.; Persans, M.W.; Nieman, K.; Albrecht, C.; Peer, W.; Pickering, I.J.; Salt, D.E. Increased Glutathione Biosynthesis Plays a Role in Nickel Tolerance in Thlaspi Nickel Hyperaccumulators. *Plant Cell* **2004**, *16*, 2176–2191. [CrossRef]
43. Bennett, L.E.; Burkhead, J.L.; Hale, K.L.; Terry, N.; Pilon, M.; Pilon-Smits, E.A.H. Analysis of transgenic Indian mustard plants for phytoremediation of metal-contaminated mine tailings. *J. Environ. Qual.* **2003**, *32*, 432–440. [PubMed]
44. Al-Rub, F.A.A.; El-Naas, M.H.; Ashour, I.; Al-Marzouqi, M. Biosorption of copper on *Chlorella vulgaris* from single, binary and ternary metal aqueous solutions. *Process Biochem.* **2006**, *41*, 457–464. [CrossRef]
45. Zhang, C.; Laipan, M.; Zhang, L.; Yu, S.; Li, Y.; Guo, J. Capturing effects of filamentous fungi Aspergillus flavus ZJ-1 on microalgae *Chlorella vulgaris* WZ-1 and the application of their co-integrated fungi-algae pellets for Cu(II) adsorption. *J. Hazard. Mater.* **2023**, *442*, 130105. [CrossRef] [PubMed]
46. Sen Gupta, S.; Bhattacharyya, K.G. Kinetics of adsorption of metal ions on inorganic materials: A review. *Adv. Colloid Interface Sci.* **2011**, *162*, 39–58. [CrossRef] [PubMed]
47. Hu, X.; Jia, L.; Cheng, J.; Sun, Z. Magnetic ordered mesoporous carbon materials for adsorption of minocycline from aqueous solution: Preparation, characterization and adsorption mechanism. *J. Hazard. Mater.* **2019**, *362*, 1–8. [CrossRef] [PubMed]
48. Shen, J.; Huang, G.; An, C.; Xin, X.; Huang, C.; Rosendahl, S. Removal of Tetrabromobisphenol A by adsorption on pinecone-derived activated charcoals: Synchrotron FTIR, kinetics and surface functionality analyses. *Bioresour. Technol.* **2018**, *247*, 812–820. [CrossRef] [PubMed]
49. Langmuir, I. The adsorption of gases on plane surfaces of glass, mica and platinum. *J. Am. Chem. Soc.* **1918**, *40*, 1361–1403. [CrossRef]
50. Musah, B.I.; Wan, P.; Xu, Y.; Liang, C.; Peng, L. Contrastive analysis of nickel (II), iron (II), copper (II), and chromium (VI) removal using modified *Chlorella vulgaris* and Spirulina platensis: Characterization and recovery studies. *J. Environ. Chem. Eng.* **2022**, *10*, 108422. [CrossRef]
51. Sayadi, M.H.; Rashki, O.; Shahri, E. Application of modified Spirulina platensis and *Chlorella vulgaris* powder on the adsorption of heavy metals from aqueous solutions. *J. Environ. Chem. Eng.* **2019**, *7*, 103169. [CrossRef]
52. Shekari, H.; Sayadi, M.H.; Rezaei, M.R.; Allahresani, A. Synthesis of nickel ferrite/titanium oxide magnetic nanocomposite and its use to remove hexavalent chromium from aqueous solutions. *Surf. Interfaces* **2017**, *8*, 199–205. [CrossRef]
53. Krishna, D.N.G.; Philip, J. Review on surface-characterization applications of X-ray photoelectron spectroscopy (XPS): Recent developments and challenges. *Appl. Surf. Sci. Adv.* **2022**, *12*, 100332. [CrossRef]
54. Fang, B.; Xu, Y.; Kawashima, H.; Hata, T.; Kijima, M. Algal carbons hydrothermally produced from Spirulina and Chlorella with the assistance of phthalaldehyde: An effective precursor for nitrogen-containing porous carbon. *Algal Res.* **2021**, *60*, 102502. [CrossRef]
55. Tan, J.; Yi, H.; Zhang, Z.; Meng, D.; Li, Y.; Xia, L.; Song, S.; Wu, L.; Sáncheze, R.M.T.; Farías, M.E. Montmorillonite facilitated Pb(II) biomineralization by Chlorella sorokiniana FK in soil. *J. Hazard. Mater.* **2022**, *423*, 127007. [CrossRef] [PubMed]
56. Gu, S.; Lan, C.Q. Effects of culture pH on cell surface properties and biosorption of Pb(II), Cd(II), Zn(II) of green alga Neochloris oleoabundans. *Chem. Eng. J.* **2023**, *468*, 143579. [CrossRef]
57. Puerto, M.A.; Costa, T.M.H.; Jornada, J.A.H.; Balzaretti, N.M. Pyrolisys of α-aminoacids under high-pressure investigated by XPS, Raman and infrared spectroscopy. *Mater. Chem. Phys.* **2018**, *211*, 107–116. [CrossRef]
58. Li, C.; Li, P.; Fu, H.; Chen, J.; Ye, M.; Zhai, S.; Hu, F.; Zhang, C.; Ge, Y.; Fortin, C. A comparative study of the accumulation and detoxification of copper and zinc in Chlamydomonas reinhardtii: The role of extracellular polymeric substances. *Sci. Total Environ.* **2023**, *871*, 161995. [CrossRef] [PubMed]
59. Sai, L.; Chen, J.; Chang, Q.; Shi, W.; Chen, Q.; Huang, L. Protein-derived carbon nanodots with an ethylenediamine-modulated structure as sensitive fluorescent probes for Cu^{2+} detection. *RSC Adv.* **2017**, *7*, 16608–16615. [CrossRef]
60. Inagaki, M.; Toyoda, M.; Soneda, Y.; Morishita, T. Nitrogen-doped carbon materials. *Carbon* **2018**, *132*, 104–140. [CrossRef]
61. Zhao, C.; Li, X.; Ding, C.; Liao, J.; Du, L.; Yang, J.; Yang, Y.; Zhang, D.; Tang, J.; Liu, N.; et al. Characterization of uranium bioaccumulation on a fungal isolate Geotrichum sp. dwc-1 as investigated by FTIR, TEM and XPS. *J. Radioanal. Nucl. Chem.* **2016**, *310*, 165–175. [CrossRef]

62. Wang, Z.; Zhang, Z.; Xia, L.; Farías, M.E.; Sánchez, R.M.T.; Belfiore, C.; Montes, M.L.; Tian, X.; Chen, J.; Song, S. Sulfate induced surface modification of Chlorella for enhanced mercury immobilization. *J. Environ. Chem. Eng.* **2022**, *10*, 108156. [CrossRef]
63. Li, G.; Ye, J.; Fang, Q.; Liu, F. Amide-based covalent organic frameworks materials for efficient and recyclable removal of heavy metal lead (II). *Chem. Eng. J.* **2019**, *370*, 822–830. [CrossRef]
64. Yuen, C.W.M.; Ku, S.K.A.; Choi, P.S.R.; Kan, C.W.; Tsang, S.Y. Determining Functional Groups of Commercially Available Ink-Jet Printing Reactive Dyes Using Infrared Spectroscopy. *Res. J. Text. Appar.* **2005**, *9*, 26–38. [CrossRef]
65. Freitas, J.; Netto, A.M.; Corrêa, M.M.; Xavier, B.T.L.; Assis, F.X. Potassium adsorption in soil cultivated with sugarcane. *An. Acad. Bras. Cienc.* **2018**, *90*, 541–555. [CrossRef] [PubMed]
66. Wang, J.; Chen, C. Biosorption of heavy metals by Saccharomyces cerevisiae: A review. *Biotechnol. Adv.* **2006**, *24*, 427–451. [CrossRef] [PubMed]
67. Doshi, H.; Ray, A.; Kothari, I.L. Bioremediation potential of live and dead Spirulina: Spectroscopic, kinetics and SEM studies. *Biotechnol. Bioeng.* **2007**, *96*, 1051–1063. [CrossRef] [PubMed]
68. Li, N.; Qin, L.; Jin, M.; Zhang, L.; Geng, W.; Xiao, X. Extracellular adsorption, intracellular accumulation and tolerance mechanisms of Cyclotella sp. to Cr(VI) stress. *Chemosphere* **2021**, *270*, 128662. [CrossRef] [PubMed]
69. Li, C.; Zheng, C.; Fu, H.; Zhai, S.; Hu, F.; Naveed, S.; Zhang, C.; Ge, Y. Contrasting detoxification mechanisms of Chlamydomonas reinhardtii under Cd and Pb stress. *Chemosphere* **2021**, *274*, 129771. [CrossRef]
70. Cheng, Y.; Zhang, T.; Chen, S.; Li, F.; Qing, R.; Lan, T.; Yang, Y.; Liao, J.; Liu, N. Unusual uranium biomineralization induced by green algae: Behavior investigation and mechanism probe. *J. Environ. Sci.* **2023**, *124*, 915–922. [CrossRef]